Vision Research 48 (2008) 2564–2568

Contents lists available at ScienceDirect

Vision Research

journal homepage: www.elsevier.com/locate/visres

In vivo imaging of the photoreceptor mosaic of a rod monochromat

Joseph Carroll [a,*], Stacey S. Choi [b], David R. Williams [c]

[a] Department of Ophthalmology, Medical College of Wisconsin, The Eye Institute, 925 North 87th Street, Milwaukee, WI 53226, USA
[b] Department of Ophthalmology & Vision Science, University of California-Davis, Sacramento, CA 95817, USA
[c] Center for Visual Science, University of Rochester, Rochester, NY 14627, USA

ARTICLE INFO

Article history:
Received 15 October 2007
Received in revised form 3 February 2008

Keywords:
Cones
Rods
Adaptive optics
Achromatopsia
Retinal disease
Waveguiding

ABSTRACT

Complete achromatopsia (i.e., rod monochromacy) is a congenital vision disorder in which cone *function* is absent or severely diminished, often due to mutations in one of two components of the cone phototransduction cascade (transducin or the cyclic-nucleotide gated channel). Previous histological data concerning cone *structure* are conflicting; suggesting anywhere from normal numbers of foveal cones to a complete absence of foveal cones. Here, we used an adaptive optics ophthalmoscope to obtain *in vivo* retinal images from a rod monochromat for whom the genetic basis of the disorder consists of a homozygous mutation in the CNGB3 gene. Behavioral data from the patient were consistent with an absence of cone function. Retinal images revealed a severely disrupted photoreceptor mosaic in the fovea and parafovea, where the size and density of the visible photoreceptors resembled that of normal rods. Imaging of additional rod monochromats to characterize differences in the photoreceptor mosaic between genetically classified patients will be required to determine which, if any, might be receptive to restorative gene therapy procedures.

1. Introduction

Rod monochromacy is a rare disorder (≈1 in 30,000) typically characterized by a lack of color discrimination, photophobia, reduced acuity, visual nystagmus, and non-detectable cone electroretinograms (ERGs) (see Hess, Sharpe, & Nordby, 1990; Pokorny, Smith, Verriest, & Pinkers, 1979, for thorough reviews). In order to account for the apparent absence of cone function, Galezowski (1868) first proposed a 'rod-only' theory in which the cones of the retina are malformed or completely absent and visual function takes place entirely in the rod photoreceptors. Subsequent histological studies partially discounted this theory, but the result is an inconsistent picture of the photoreceptor mosaic of the achromat. Larsen (1921) reported scarce, malformed retinal cones in the fovea and normal peripheral cones in the retina of a 29-year-old female. Harrison, Hoefnagel, and Hayward (1960) found imperfectly shaped and reduced numbers of cones throughout the retina of a 19-year-old male. In the retina of a 69-year-old female, Falls, Wolter, and Alpern (1965) observed normal numbers of odd-shaped foveal cones and scarce numbers in the periphery. Most recently, Glickstein and Heath (1975) found no evidence of cones in the fovea and reduced numbers of cones elsewhere in the retina of an 85-year-old male. Thus, the question of the composition of photoreceptors in the complete achromat remains open.

The discovery of the genetic basis of complete achromatopsia both clarified and complicated the attempts to elucidate the photoreceptor complement in these individuals. Complete achromatopsia has been linked to numerous mutations in CNGA3 and CNGB3 (which encode the α- and β-subunits, respectively, of the cone cyclic-nucleotide gated (CNG) channel), as well as GNAT2, which encodes the α-subunit of the cone G-protein transducin. There is corresponding data demonstrating enormous phenotypic variability in the disease (Eksandh, Kohl, & Wissinger, 2002; Johnson et al., 2004; Khan, Wissinger, Kohl, & Sieving, 2007; Nishiguchi, Sandberg, Gorji, Berson, & Dryja, 2005; Träkner et al., 2004). The genetic variation likely underlies at least part of the phenotypic differences and might even explain the discrepant histological reports, however, a systematic linkage of genotype and phenotype has not been done.

There has been renewed interest in the retina of the congenital achromat, due largely to the development of non-invasive, high-resolution, *in vivo* imaging modalities (Anger et al., 2004; Liang, Williams, & Miller, 1997; Pircher & Zawadzki, 2007; Roorda et al., 2002; Zhang, Rha, Jonnal, & Miller, 2005), together with the development of novel gene therapy approaches to restoring cone function in animal models of the disease (Alexander et al., 2007; Komaromy et al., 2007). While the typical monochromat fundus is normal (though see Khan et al., 2007), cellular details in the retina can now be detected with other imaging modalities.

Abbreviations: CNG, cyclic-nucleotide gated; OCT, optical coherence tomography; ERG, electroretinogram; AO, adaptive optics

* Corresponding author. Fax: +1 414 456 6690.
E-mail address: jcarroll@mcw.edu (J. Carroll).

0042-6989/$ - see front matter © 2008 Elsevier Ltd. All rights reserved.
doi:10.1016/j.visres.2008.04.006

Recently, optical coherence tomography (OCT) images of patients with achromatopsia revealed an absence of photoreceptor reflectivity in the fovea, and this was interpreted as being due to an absence of healthy cone photoreceptors (Barthelmes et al., 2006; Varsányi, Somfai, Lesch, Vámos, & Farkas, 2007), though the two studies differ on the abnormality of foveal thickness in achromats. Moreover, Nishiguchi et al. (2005) detected a normal layer of photoreceptors using OCT in a subset of achromats with CNGB3 mutations. Despite their wide clinical use, commercial OCT scans offer limited resolution of the photoreceptor layer (though averaging multiple frames can enhance these images; Sander, Larsen, Thrane, Hougaard, & Jørgensen, 2005). Thus, it is difficult to draw firm conclusions about the photoreceptor complement of rod monochromats.

By correcting for the eye's optical aberrations, an adaptive optics (AO) fundus camera enables direct visualization of the photoreceptor mosaic *in vivo* (Liang et al., 1997). This imaging tool has been used to study both the normal retina (Miller, Williams, Morris, & Liang, 1996; Roorda, Metha, Lennie, & Williams, 2001; Roorda et al., 2002) and the diseased retina (Carroll, Neitz, Hofer, Neitz, & Williams, 2004; Choi et al., 2006; Duncan et al., 2007; Roorda, 2000; Wolfing, Chung, Carroll, Roorda, & Williams, 2006). Here, we imaged the retina of an achromat (of known genotype) in order to characterize the photoreceptor mosaic. This imaging approach is likely to yield benefit in characterizing the photoreceptor complement in other retinal degenerations, especially in those where restorative therapies are being developed.

2. Methods

2.1. Subjects

Subjects provided informed consent after the nature and possible consequences of the study were explained. All research adhered to the tenets of the Declaration of Helsinki, and study protocols were approved by the institutional research board at the University of Rochester. A male (ACH0016) diagnosed with complete achromatopsia (age 28) and his mother (ACH0015), a carrier (age 50), were recruited for this study. Complete ophthalmologic examinations were performed on both subjects just prior to retinal imaging, which was performed over a 2-day period. Color vision was assessed using a variety of tests, including the Rayleigh match, pseudoisochromatic plates (AO-HRR, Dvorine and Ishihara) and the Neitz test of color vision. DNA analysis was done previously, revealing that ACH0016 was homozygous for the common 1 base pair deletion (1148 del C) in the CNGB3 subunit of the cone CNG channel and his mother (ACH0015) was heterozygous for the mutation. (Dr. Irene Maumenee, personal communication). This mutation results in a frame-shift downstream of amino acid Threonine383 and introduces a premature stop codon, which is effectively a null allele (Peng, Rich, & Varnum, 2003).

2.2. Adaptive optics imaging

Images of the photoreceptor mosaic were obtained using an AO-fundus camera (see Hofer et al., 2001; Putnam et al., 2005, for a schematic and system details). The subjects' right eye was dilated and accommodation paralyzed through use of a combination of Phenylephrine Hydrochloride (2.5%) and Tropicamide (1%). The head was stabilized using a dental impression on a bite bar. In a continuous closed loop, we measured the eye's monochromatic aberrations over a 6.8-mm pupil with a Shack-Hartmann wavefront sensor and corrected for them until the root-mean-square wavefront error fell below 0.1 μm or after 800 ms elapsed, whichever happened first. Additional details on wavefront measurement and compensation have been previously published. Once a wavefront correction was obtained, a retinal image was acquired by illuminating the retina with a 1° diameter, 4-ms flash (630, 25 nm bandwidth; full width at half maximum) from a krypton arc flash lamp. The short duration of the flash helped to minimize the effects of motion blur on the accompanying retinal image. A circular fixation target (front-illuminated with a dim long-wavelength light) was used to record the relative retinal location of each image.

2.3. Image analysis

Images from the same retinal location were registered with subpixel accuracy (accounting for translation and rotation) and averaged using a custom MatLab (MathWorks, Natick, MA) image registration program (Putnam et al., 2005). We summated between 3 and 12 individual frames to create each of the images used for analysis. Cone density was calculated using previously published methods (Carroll et al., 2004) as well as a modified version of a software program that has been used to automatically identify photoreceptors in AO retinal images (Li & Roorda, 2007). Image J (NIH, Bethesda, MD) was used to measure photoreceptor diameters (Abramoff, Magelhaes, & Ram, 2004). This was done by examining the plot profile of 30 pseudo-randomly selected cells from each image (see Fig. 2c). An axial length measurement from the Zeiss IOL Master (Dublin, CA) was used to derive a retinal magnification for the images as described by Bennett, Rudnicka, and Edgar (1994).

3. Results

3.1. Clinical phenotype

Dilated fundus examination of ACH0016 revealed mild RPE atrophy OU and a blond fundus consistent with the patient's complexion. There was a loculated area of subretinal fluid (not involving the foveal center—inferonasal macula, OS), consistent with central serous retinopathy. Best-corrected visual acuity was 20/150. Dilated fundus examination of ACH0015 showed multiple small drusen OU, not uncommon for her age. Color vision tests were normal for ACH0015, whereas ACH0016 showed a complete lack of color discrimination. Both rod- and cone-based ERG's were normal for ACH0015, while there was no detectable cone response from ACH0016 (although rod amplitudes were normal).

3.2. Adaptive optics imaging

Images for ACH0016 were obtained at 1.25°, 2.5°, 4°, and 10° temporal from fixation (OD). Numerous photoreceptors are visible in all four images, though the photoreceptor mosaic is severely disrupted compared to images from a normal retina (Fig. 1). The density of the photoreceptors was consistent with normal rod, not cone, densities (see Table 1). Normal cone density peaks in the fovea and declines rapidly moving away from the fovea, whereas rod photoreceptors are absent in the central fovea and reach a maximum density near 10° eccentricity (Curcio, Sloan, Kalina, & Hendrickson, 1990). The photoreceptor density for the achromat examined in this study remained relatively constant between the 1.25° and 4° images, though there was a slight elevation at 10°. Images from the heterozygous carrier mother (at 1.25° and 2.5°, OD) revealed no obvious disruption. An analysis of her retinal images revealed a continuous mosaic in which the photoreceptors were of a density characteristic of cones (Table 1).

Fig. 2a shows an image from 10° temporal from fixation for ACH0016. Remarkably, despite only two frames being used to create this image, photoreceptor structure is clearly resolved. Moreover, at a location where rods outnumber cones in the normal retina by nearly 10:1, we observe a high density of cells. In order to further probe their identity, we measured the cell diameter in this image as well as the other three locations imaged. Shown in Fig. 2b is a plot of cell diameter as a function of retinal eccentricity. At 10° retinal eccentricity, typical rod diameter is 2 μm, while cones are nearly 8 μm in diameter (Samy & Hirsch, 1989). The average (± SEM) diameter of the structures in the image in Fig. 2a is 2.99 ± 0.092 μm. This is larger than the calculated full-width half-height (FWHH) of the point spread function of the optical system (6.8 mm pupil, 630 nm), therefore we are confident that these structures are not smaller than the actual measurement. Fig. 2c shows 2D plot profiles from three different locations in the image in Fig. 2a. The individual profiles have been translated vertically for visibility, but it illustrates that even in our worst image it is quite easy to obtain robust estimates of cell diameter.

Achromats typically have nystagmus and poor fixation (Sharpe, Collewijn, & Nordby, 1986), though ACH0016 had minimal nystagmus and fairly reliable fixation (this can be assessed by the displacement of successive retinal images from a given reference frame). Moreover, we were able to return to image the same retinal

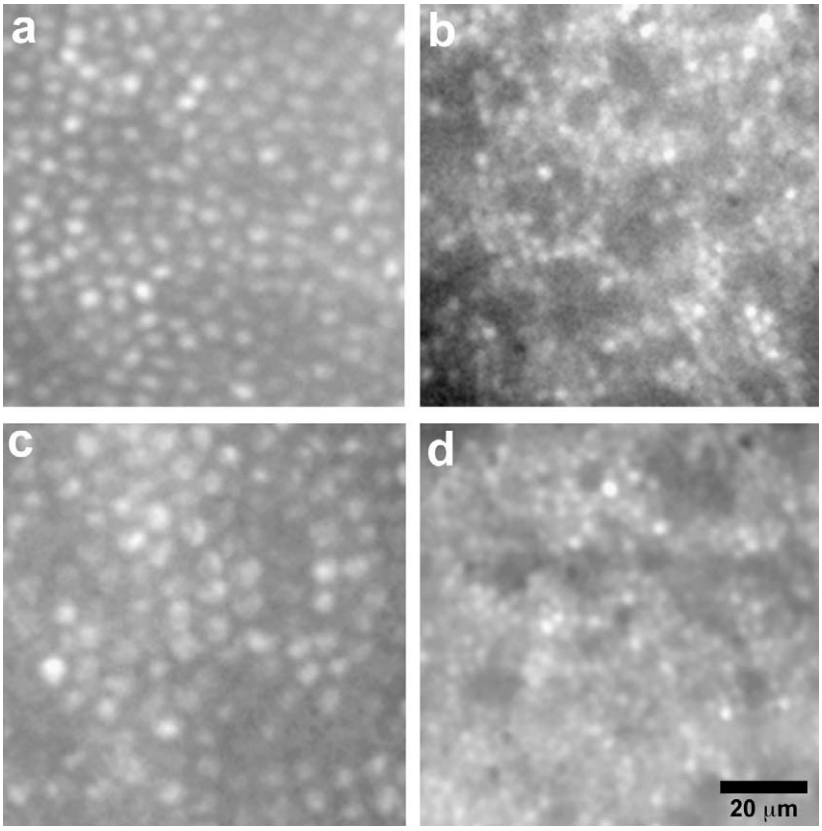

Fig. 1. Images of the *in vivo* photoreceptor mosaic. (a and c) Images from a 28-year-old normal male, who had been imaged as part of a number of unrelated studies over the course of 3 months. (b and d) Images from a 28-year-old rod monochromat. Images are from 2.5° (a and b) and 4° (c and d) temporal retina. Scale bar is 20 μm.

Table 1
Cone and rod density in normals and a rod monochromat

	1.25°	2.5°	4°	10°
AOCH0016	55,466	49,300	52,322	82,990
AOCH0015	49,323	26,539	ND	ND
Normal cone (Curcio et al., 1990)	46,086	26,215	20,699	8559
Normal cone AO	44,330	23,362	15,675	7656
Normal rod (Curcio et al., 1990)	22,032	54,542	78,011	129,920

All values are in cells/mm^2.

location on subsequent days, consistent with reliable fixation. However, even though fixation was sufficiently reliable for image registration, another potential source of error comes from the observation that achromats often adopt preferred fixation locations away from the fovea. Thus, the absolute retinal location of the images from our achromat might be displaced by up to 2° (cf. Baseler et al., 2002). Nevertheless, the *relative* position of our imaging locations seems reliable, and thus the interpretation that the photoreceptors in the images from the monochromat are rods remains the most parsimonious.

4. Discussion

Here, we present the first *in vivo* images of the photoreceptor mosaic of a rod monochromat. At four different retinal locations along the temporal meridian, images from the monochromat revealed a severely disrupted photoreceptor mosaic. Moreover, the size and density of the visible cells were typical for rod, not cone, photoreceptors. These results suggest that, at least in this achromat, the retina is largely devoid of healthy cone photoreceptors. The intermittent gaps in the mosaic could be the result of either absence of cone development or cone degeneration. It seems likely, given the available histological data (and the small patches of retina imaged here), that there could be residual cone structure elsewhere in this patient's retina. In the normal retina, cones are easily imaged with adaptive optics as a result of their strong waveguide nature (Roorda & Williams, 2002). Thus, if cones *were* present at the locations we imaged, they are damaged to the point that they are not functioning (given the ERG data in this patient) and not visible in the retinal images (likely due to impaired waveguiding—i.e., lack of an outer segment).

While unlikely, an alternate interpretation of our data is of course that the photoreceptors in these images are morphologically and topographically abnormal cones. Such cones could not be functioning, given the patient's phenotype as a complete achromat (nondetectable cone ERG, no color discrimination, photophobia, nystagmus, and his homozygous CNGB3 null mutation). As mentioned above, an interpretation of the current data might suggest that achromats with different causative mutations can have varying levels of residual cone function. We suspect that imaging such individuals with AO ophthalmoscopy will reveal significant differences in their photoreceptor mosaics that correlate with the degree of residual cone function. Furthermore, examination of genetically classified patients with high-resolution retinal imaging is likely to provide valuable insight into pathogenesis of the disease as well as identify those individuals who might be most receptive to newly developed gene therapies (Alexander et al., 2007; Komaromy et al., 2007).

If as we believe these photoreceptors are rods, one wonders why they are not as easily visualized in the normal retina under similar imaging conditions. To our knowledge, there is only one report of *in vivo* images of rods from the normal human retina. In high-resolution retinal images taken 15–20° from fixation in the normal retina, Choi and colleagues observed a continuous cone

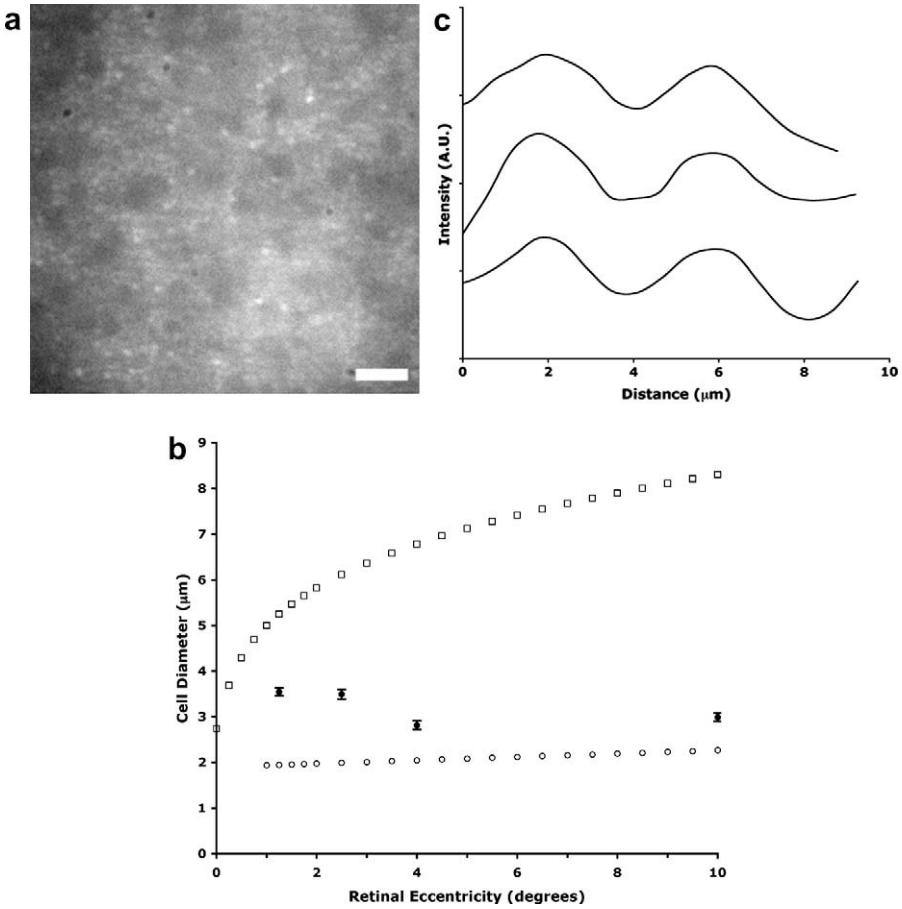

Fig. 2. Cell size as a function of eccentricity. (a) Retinal image from 10° eccentricity from AOCH0016. Scale bar is 20 μm. (b) Diameters of rods (*open circles*) and cones (*open squares*) as a function of retinal eccentricity for the normal human retina (data from Samy & Hirsch, 1989). Filled circles are average data from subject AOCH0016, error bars represent ±1 SEM. (c) Three separate plot profiles from (a), translated on the *y*-axis for easier visualization.

mosaic with numerous rods intermingled throughout the image (Choi et al., 2004). The difficulty in imaging them, and the relative sparseness at retinal locations where they should outnumber the cones nearly 10-fold, is consistent with previous data that rods are less effective waveguides than cones (Alpern, Ching, & Kithara, 1983; van Loo & Enoch, 1975). It may be that this is only a limiting factor when trying to image the *normal* retina, where the light from the cones may be reducing the contrast of the interleaved rods. Another possibility is that while in the normal retina cones are thought to have more mitochondria than rods (Hoang, Linsenmeier, Chung, & Curcio, 2002), the rods in the monochromat retina might be more active due to a change in lifestyle and as a result, the rods would have an increased metabolic demand. This might result in an increase in the relative difference in refractive index, rendering them more efficient waveguides and easier to visualize with this particular imaging technique. Alternatively, the absence of cone photoreceptors in this retina may have allowed the remaining rods to swell, as has been reported to occur when rods are lost in normal aging (Curcio, 2001). Indeed, while the photoreceptors imaged are more consistent with rod, rather than cone, diameters, they are slightly larger than values proposed in the literature (Samy & Hirsch, 1989). Even a slight increase in size would greatly improve the ability to resolve them in the AO images, so further work remains in determining what mechanisms are acting to increase rod contrast in this retina.

Finally, the phenotypic variability in genetically identical achromats indicates that there are other mitigating factors that influence the degree of residual cone structure and function in a given rod monochromat will have. This underscores the importance of imaging the retinae of individual subjects rather than making general assumptions about the achromat retina. Moreover, Jacobson et al. (2005) prophetically stated that "...identifying and then targeting retinal locations with retained photoreceptors will be a prerequisite for successful gene therapy in humans...". This is worth reiterating, with the cautionary note that the story of cone survival in the mouse and dog models of achromatopsia may not hold for all human achromats. Fortunately, both the therapeutic and diagnostic tools exist for us to proceed with prudence in the quest to restore cone function to congenital rod monochromats.

Acknowledgments

We thank L. Chen, M. Chung, N. Doble, I. H. Maumenee, J. Morgan, and J. Porter for their assistance. We acknowledge financial support from the National Eye Institute (F32-EY014749 to J.C., and P30-EY001319 and R01-EY004367 to D.R.W.), The Steinbach Foundation (to S.S. and D.R.W.), Fight for Sight (to J.C.), and an unrestricted Research to Prevent Blindness Award (Medical College of Wisconsin). J.C. is the recipient of a Research to Prevent Blindness Career Development Award. This work has been supported in part by the National Science Foundation Science and Technology Center for Adaptive Optics, managed by the University of California at Santa Cruz under co-operative agreement No. AST-9876783.

References

Abramoff, M. D., Magelhaes, P. J., & Ram, S. J. (2004). Image processing with ImageJ. *Biophotonics International, 11*(7), 36–42.

Alexander, J. J., Umino, Y., Everhart, D., Chang, B., Min, S. H., Li, Q., et al. (2007). Restoration of cone vision in a mouse model of achromatopsia. *Nature Medicine, 13*(6), 685–687.

Alpern, M., Ching, C. C., & Kithara, K. (1983). The directional sensitivity of retinal rods. *Journal of Physiology, 343*, 577–592.

Anger, E. M., Unterhuber, A., Hermann, B., Sattmann, H., Schubert, C., Morgan, J. E., et al. (2004). Ultrahigh resolution optical coherence tomography of the monkey fovea. Identification of retinal sublayers by correlation with semithin histology sections. *Experimental Eye Research, 78*, 1117–1125.

Barthelmes, C., Sutter, F. K., Kurz-Levin, M. M., Bosch, M. M., Helbig, H., Niemeyer, G., et al. (2006). Qualitative analysis of OCT characteristics in patients with achromatopsia and blue-cone monochromatism. *Investigative Ophthalmology & Visual Science, 47*(3), 1161–1166.

Baseler, H. A., Brewer, A. A., Sharpe, L. T., Morland, A. B., Jägle, H., & Wandell, B. A. (2002). Reorganization of human cortical maps caused by inherited photoreceptor anomalies. *Nature Neuroscience, 5*, 364–370.

Bennett, A. G., Rudnicka, A. R., & Edgar, D. F. (1994). Improvements on Littmann's method of determining the size of retinal features by fundus photography. *Graefe's Archive for Clinical and Experimental Ophthalmology, 232*, 361–367.

Carroll, J., Neitz, M., Hofer, H., Neitz, J., & Williams, D. R. (2004). Functional photoreceptor loss revealed with adaptive optics: An alternate cause for color blindness. *Proceedings of the National Academy of Sciences of the United States of America, 101*(22), 8461–8466.

Choi, S. S., Doble, N., Christou, J., Plandowski, J., Enoch, J., & Williams, D. (2004). In vivo imaging of the human rod photoreceptor mosaic. *Investigative Ophthalmology & Visual Science, 45*. E-Abstract 2794.

Choi, S. S., Doble, N., Hardy, J. L., Jones, S. M., Keltner, J. L., Olivier, S. S., et al. (2006). In vivo imaging of the photoreceptor mosaic in retinal dystrophies and correlations with visual function. *Investigative Ophthalmology & Visual Science, 47*(5), 2080–2092.

Curcio, C. A. (2001). Photoreceptor topography in ageing and age-related maculopathy. *Eye, 15*, 376–383.

Curcio, C. A., Sloan, K. R., Kalina, R. E., & Hendrickson, A. E. (1990). Human photoreceptor topography. *The Journal of Comparative Neurology, 292*, 497–523.

Duncan, J. L., Zhang, Y., Gandhi, J., Nakanishi, C., Othman, M., Branham, K. E. H., et al. (2007). High-resolution imaging with adaptive optics in patients with inherited retinal degeneration. *Investigative Ophthalmology & Visual Science, 48*, 3283–3291.

Eksandh, L., Kohl, S., & Wissinger, B. (2002). Clinical features of achromatopsia in Swedish patients with defined genotypes. *Ophthalmic Genetics, 23*(2), 109–120.

Falls, H. F., Wolter, R., & Alpern, M. (1965). Typical total monochromasy—A histological and psychophysical study. *Archives of Ophthalmology, 74*, 610–616.

Galezowski, X. (1868). *Du diagnostic des Maladies des Yeux par la Chromatoscopie rétinienne: Précéde d'une Etude sur les Lois physiques et physiologiques des Couleurs*. Paris: J.B. Baillière et Fils.

Glickstein, M., & Heath, G. G. (1975). Receptors in the monochromat eye. *Vision Research, 15*, 633–636.

Harrison, R., Hoefnagel, D., & Hayward, J. N. (1960). Congenital total color blindness, a clinicopathological report. *Archives of Ophthalmology, 64*, 685–692.

Hess, R. F., Sharpe, L. T., & Nordby, K. (1990). *Night vision: Basic, clinical and applied aspects* (p. 550). Cambridge: Cambridge University Press.

Hoang, Q. V., Linsenmeier, R. A., Chung, C. K., & Curcio, C. A. (2002). Photoreceptor inner segments in monkey and human retina: Mitochondrial density, optics, and regional variation. *Visual Neuroscience, 19*, 395–407.

Hofer, H., Chen, L., Yoon, G. Y., Singer, B., Yamauchi, Y., & Williams, D. R. (2001). Improvement in retinal image quality with dynamic correction of the eye's aberrations. *Optics Express, 8*(11), 631–643.

Jacobson, S. G., Aleman, T. S., Cideciyan, A. V., Sumaroka, A., Schwartz, S. B., Windsor, E. A. M., et al. (2005). Identifying photoreceptors in blind eyes caused by RPE65 mutations: Prerequisite for human gene therapy success. *Proceedings of the National Academy of Sciences of the United States of America, 102*(17), 6177–6182.

Johnson, S., Michaelides, M., Aligianis, I. A., Ainsworth, J. R., Mollon, J. D., Maher, E. R., et al. (2004). Achromatopsia caused by novel mutations in both CNGA3 and CNGB3. *Journal of Medical Genetics, 41*(2), e20.

Khan, N. W., Wissinger, B., Kohl, S., & Sieving, P. (2007). CNGB3 achromatopsia with progressive loss of residual cone function and impaired rod-mediated function. *Investigative Ophthalmology & Visual Science, 48*(8), 3864–3871.

Komaromy, A. M., Alexander, J. J., Chiodo, V. A., Hauswirth, W. W., Acland, G. M., & Aguirre, G. D. (2007). Cone-directed gene therapy with rAAV leads to restoration of cone function in a canine model of achromatopsia. *Investigative Ophthalmology & Visual Science, 48*. E-Abstract 4614.

Larsen, H. (1921). Demonstration mikroskopischer Präparate von einem monochromatischen Auge. *Klinische monatsblätter für augenheilkunde, 67*, 301–302.

Li, K. Y., & Roorda, A. (2007). Automated identification of cone photoreceptors in adaptive optics retinal images. *Journal of the Optical Society of America A, 24*(5), 1358–1363.

Liang, J., Williams, D. R., & Miller, D. (1997). Supernormal vision and high-resolution retinal imaging through adaptive optics. *Journal of the Optical Society of America A, 14*(11), 2884–2892.

Miller, D. T., Williams, D. R., Morris, G. M., & Liang, J. (1996). Images of cone photoreceptors in the living human eye. *Vision Research, 36*, 1067–1079.

Nishiguchi, K. M., Sandberg, M. A., Gorji, N., Berson, E. L., & Dryja, T. P. (2005). Cone cGMP-gated channel mutations and clinical findings in patients with achromatopsia, macular degeneration, and other hereditary cone diseases. *Human Mutation, 25*, 248–258.

Peng, C., Rich, E. D., & Varnum, M. D. (2003). Achromatopsia-associated mutation in the human cone photoreceptor cyclic nucleotide-gated channel CNGB3 subunit alters the ligand sensitivity and pore properties of heteromeric channels. *The Journal of Biological Chemistry, 278*(36), 34533–34540.

Pircher, M., & Zawadzki, R. J. (2007). Combining adaptive optics with optical coherence tomography: Unveiling the cellular structure of the human retina in vivo. *Expert Review of Ophthalmology, 2*(6), 1019–1035.

Pokorny, J., Smith, V. C., Verriest, G., & Pinkers, A. J. L. (1979). *Congenital and acquired color vision defects*. *Current ophthalmology monographs*. New York: Grune and Stratton.

Putnam, N. M., Hofer, H. J., Doble, N., Chen, L., Carroll, J., & Williams, D. R. (2005). The locus of fixation and the foveal cone mosaic. *Journal of Vision, 5*(7), 632–639.

Roorda, A. (2000). Adaptive optics ophthalmoscopy. *Journal of Refractive Surgery, 16*, S602–S607.

Roorda, A., Metha, A. B., Lennie, P., & Williams, D. R. (2001). Packing arrangement of the three cone classes in primate retina. *Vision Research, 41*, 1291–1306.

Roorda, A., Romero-Borja, F., Donnelly, W. J., III, Quenner, H., Hebert, T. J., & Campbell, M. C. W. (2002). Adaptive optics scanning laser ophthalmoscopy. *Optics Express, 10*(9), 405–412.

Roorda, A., & Williams, D. R. (2002). Optical fiber properties of individual human cones. *Journal of Vision, 2*(5), 404–412.

Samy, C. N., & Hirsch, J. (1989). Comparison of human and monkey retinal photoreceptor sampling mosaics. *Visual Neuroscience, 3*, 281–285.

Sander, B., Larsen, M., Thrane, L., Hougaard, J. L., & Jørgensen, T. M. (2005). Enhanced optical coherence tomography imaging by multiple scan averaging. *British Journal of Ophthalmology, 89*, 207–212.

Sharpe, L. T., Collewijn, H., & Nordby, K. (1986). Fixation, pursuit and optokinetic nystagmus in a complete achromat. *Clinical Vision Science, 1*, 39–49.

Träkner, D., Jägle, H., Kohl, S., Apfelstedt-Sylla, E., Sharpe, L. T., Kaupp, U. B., et al. (2004). Molecular basis of an inherited form of incomplete achromatopsia. *The Journal of Neuroscience, 24*(1), 138–147.

van Loo, J. A., & Enoch, J. M. (1975). The scoptopic Stiles-Crawford effect. *Vision Research, 15*, 1005–1009.

Varsányi, B., Somfai, G. M., Lesch, B., Vámos, R., & Farkas, Á. (2007). Optical coherence tomography of the macula in congenital achromatopsia. *Investigative Ophthalmology & Visual Science, 48*(5), 2249–2253.

Wolfing, J. I., Chung, M., Carroll, J., Roorda, A., & Williams, D. R. (2006). High-resolution retinal imaging of cone-rod dystrophy. *Ophthalmology, 113*(6), 1014–1019.

Zhang, Y., Rha, J. T., Jonnal, R. S., & Miller, D. T. (2005). Adaptive optics parallel spectral domain optical coherence tomography for imaging the living retina. *Optics Express, 13*(12), 4792–4811.